

Development of an immunogenomics-based prognostic index model of laryngeal squamous cell carcinoma

Yujie Shen

Nanjing Medical University

Han Zhou

Nanjing Medical University

Shikun Dong

Nanjing Medical University

Meiping Lu

Nanjing Medical University

Weida Dong

Nanjing Medical University

Liqing Zhang (✉ 18651811663@163.com)

Nanjing Medical University

Research article

Keywords: laryngeal squamous cell carcinoma, immunotherapy

Posted Date: August 17th, 2020

DOI: <https://doi.org/10.21203/rs.3.rs-56339/v1>

License:   This work is licensed under a Creative Commons Attribution 4.0 International License.

[Read Full License](#)

Abstract

Background: The immune system greatly affects the prognosis of various malignancies. Studies on differentially expressed immune-related genes (IRGs) in the immune microenvironment of laryngeal squamous cell carcinoma (LSCC) have rarely been reported.

Methods: In this paper, the prognostic potentials of IRGs in LSCC were explored. The RNAseq dataset containing differentially expressed IRGs and corresponding clinical information of LSCC patients was obtained from The Cancer Genome Atlas (TCGA). A total of 371 up-regulated and 61 down-regulated IRGs were identified. Subsequent functional enrichment analysis revealed that the pathway of IRGs was mainly enriched in the cytokine-cytokine receptor interaction. Then, 30 IRGs with prognostic potentials in LSCC were screened out, and the regulatory network induced by relevant transcription factors (TFs) were constructed.

Results: Finally, multivariate Cox regression analysis was conducted to assess the prognostic potential of 15 IRGs after adjustment of clinical factors and LSCC patients were classified into 2 subgroups based on different outcomes. The gene expression of the model was verified by other independent databases. Nomogram including the 15 IRGs signature was established and shown some clinical net benefit. Intriguingly, B cells were significantly enriched in the low-risk group.

Conclusion: These findings may contribute to the development of potential therapeutic targets and biomarkers for the new-immunotherapy of LSCC.

1 Background

Laryngeal cancer, a most common malignant tumors in the head and neck, ranks the eleventh among the most common malignant tumors in men[1]. Notably, patients with invasive and metastatic laryngeal cancer have a poor prognosis. More than 95% cases of laryngeal cancer are laryngeal squamous cell carcinoma (LSCC). Despite great strides on LSCC treatment in recent years, the mortality rate of LSCC remains high [2]. Due to the lack of symptoms, LSCC in the early stage is often neglected. Furthermore, because of the screening and diagnostic limitations, the detective rate of LSCC, especially early-stage LSCC, is relatively low. Therefore, identifying effective biomarkers and target genes is of vital importance in improving diagnostic and therapeutic efficacies for LSCC [3].

Previous studies have confirmed the significance of tumor immunoreaction in the tumor microenvironment. Prognostic signatures based on immune-related genes (IRGs) have been proposed for nonsquamous non-small cell lung cancer [4] and papillary thyroid cancer [5]. Tumor-infiltrating immune cells with different densities, localizations and types have been identified as prognostic factors in lung cancer [6], colorectal cancer[7] and breast cancer[8]. Nevertheless, the clinical relevance and prognostic significance of IRGs in LSCC are yet to be elucidated.

Herein, we aimed to explore potential therapeutic targets and biomarkers for immunotherapy of LSCC. TCGA datasets containing IRG expression profiles and clinical information of LSCC patients were first analyzed. An immunogenomics-based prognostic index of LSCC was developed and the potential mechanism was further discussed.

2 Methods

2.1 Clinical samples and data acquisition

We downloaded the RNAseq dataset with mRNA level 3 and corresponding clinical information from The Cancer Genome Atlas (TCGA)—the largest cancer gene information database to collect relevant data, including the expression profiles and clinical information of 12 laryngeal tissues and 111 LSCC samples, from different microarray platforms[9] for further analyses. We also obtained a list of IRGs via the Immunology Database and Analysis Portal (ImmPort) database (<https://www.immport.org>)[10]. At the same time, the list of tumor-related transcription factors (TFs) was obtained from Cistrome Cancer (<http://cistrome.org/>)[11]—a comprehensive resource of transcriptional and epigenetic factors regulating abnormal gene expression patterns in cancers. Finally, the abundance of six types of tumor-infiltrating immune cells in LSCC was retrieved from Tumor IMMune Estimation Resource (TIMER) (<https://cistrome.shinyapps.io/timer/>) [12].

2.2 Differential expressed genes (DEGs) analysis

We identified DEGs between LSCC and normal tissues via R software (version: x64 3.2.1) and package Limma[13]. The screening criteria were: $|\log(\text{FC})| \geq 1$ and $\text{adj.p} < 0.05$.

2.3 Identification of immune-related genes (IRGs)

IRGs were then identified from the intersection between all differentially expressed genes and immune-related genes. To explore the potential molecular mechanisms of the IRGs, we performed Gene Ontology(GO)enrichment analysis and the Kyoto Encyclopedia of Genes and Genomes (KEGG) signaling pathway analysis on these differentially expressed IRGs using package Cluster profiler of R.

2.4 Survival analysis and construction of regulatory network

Prognostic IRGs were selected by univariate Cox analysis using the package survival in R. At the same time, TFs were obtained from Cistrome. Then, we screened differentially expressed TFs from these TFs by package limma in R software with $\text{adj.p} < 0.05$ and $|\log(\text{FC})| \geq 1$. The regulatory network was constructed based on clinically relevant TFs and filtered TFs with a standard of correlation coefficient more than 0.3 and $p < 0.05$. The results of the interaction were imported into Cytoscape 3.7.1[14] to establish a regulatory network to explore role of TFs in regulating these prognostic IRGs.

2.5 Construction of a prognostic index model of LSCC based on immune-related genes

We constructed a prognostic index model based on the result of the multivariate Cox regression analysis of prognostic IRGs.

2.6 External validation of the gene expression

We collected high-throughput gene expression dataset, numbered GSE59102, from the GEO database[15]. Background correction, standardization and expression value calculation were performed on the original dataset using package Impute and Limma of R software and $\text{adj.}p\text{-val} < 0.05$ were defined as the screening criteria. The protein expression of the genes in the prognostic gene signature was explored in the Human Protein Atlas database[16].

2.7 Verification the prognostic capacity of prognostic index

Patients were divided into the high-risk group and the low-risk group based on the median risk score value. ROC curves were constructed via the package survival ROC in R to validate the performance of prognostic index[17]. Survival analysis of two groups with a threshold of $p < 0.05$ was carried out by package survival and survminer in R to verify the clinical efficacy. In addition, we observed the prognostic value of prognostic index by introducing clinical factors like age and grade. Clinical survival analysis based subgroup was also conducted and a value of $p < 0.05$ was considered significant statistically.

2.8 Building and validating a predictive nomogram

We took the all independent prognostic factors identified by multivariate Cox regression analysis into a nomogram to investigate the likelihood of 1-OS, 3-OS and 5-OS for LSCC. The effectiveness of the nomogram was evaluated by discrimination and calibration. Finally, we plotted the calibration curve of the nomogram by package(rms) of R to observe the relationship between the predicted probability of the nomogram and the observed rate.

2.9 Functional enrichment analysis

We used Gene Set Enrichment Analysis (GSEA) [18] to identify consistent differences between high-risk and low-risk groups and to explore possible biological processes. In the gene list of KEGG, $p < 0.05$ were considered to be statistically significant screening criteria.

2.10 Differential expression of tumor-infiltrating immune cells between high-risk and low-risk groups We obtained immune infiltrate levels of LSCC patients from TIMER and calculated differential expression of tumor-infiltrating immune cells between high-risk and low-risk groups using two-sample T-test.

3. Results

3.1 Analyses on DEGs

Analyses on 5483 DEGs were performed in R, and a total of 4611 up-regulated and 872 down-regulated DEGs were identified (Fig. 1).

3.2 Identification of IRGs

A total of 371 up-regulated and 61 down-regulated IRGs were identified from the DEGs obtained.

Cluster analyses on IRGs were presented in Fig. 2A. As expected, GO enrichment analysis (Fig. 2B) indicated that leukocyte migration was the most significantly affected biological process (BP). The external side of plasma membrane was the most significantly affected cell composition (CC). Meanwhile, the receptor ligand activity was the most significantly affected molecular function (MF). Subsequently, the KEGG signaling pathway analysis (Fig. 2C) found that the cytokine-cytokine receptor interaction pathway was most frequently implicated. Taken together, these results suggested that differentially expressed IRGs were of significance in the development of LSCC.

3.3 Survival analysis and construction of regulatory network

After integrating clinical information from TCGA and analyzing using the univariate Cox regression, 30 prognostic IRGs were identified. Forest plots (Fig. 3) showed that 11 IRGs may be the protective factors of LSCC, while the remaining 19 IGs could be risk factors of LSCC. To investigate the regulatory mechanisms of the prognostic IRGs, expression levels of 318 TFs were examined. There were 65 differentially expressed TFs between LSCC and normal samples (Fig. 4). A regulatory network was constructed to depict these IRGs with relevant TFs (Fig. 4C).

3.4 Construction of a prognostic index model

Based on the results of the multivariate Cox regression analyses on the 15 prognostic IRGs, a prognostic index model was constructed (Table 1). Risk score of each IRG was calculated as follows:

$$\text{Risk score} = \text{Expression level of RBP1} \times 0.014515146 + \text{TLR2} \times 0.070374413 + \text{PAEP} \times 0.191308583 + \text{AHNAK} \times 0.009241029 + \text{AQP9} \times 0.109852371 + \text{CCL2} \times 0.064247745 + \text{PPARG} \times 0.249274658 + \text{CYSLTR2} \times (-1.286172307) + \text{FPR2} \times (-0.740033285) + \text{BTC} \times 0.712705592 + \text{EPO} \times (-0.896454065) + \text{STC2} \times 0.055003634 + \text{TNFRSF4} \times (-0.164413327) + \text{FCGR3B} \times 0.296296184 + \text{PLCG1} \times (-0.285536942)$$

3.5 External validation of the expression of the 15 genes

The mRNA expression of genes of the model was consistent with the results in the TCGA cohort (Table 2), yet the upregulation of PAEP and CYSLTR2 was not found in GSE59102 (Table 3). We further explored the protein expression of the genes in the Human Protein Profiles, which was shown in Fig. 5. However, we did not find the protein expression of BTC, FCGR3B and TLR2 in THPA.

3.6 Verification the prognostic capacity of the prognostic index model

LSCC patients were separated into the high-risk group and the low-risk group based on the median level of risk score (Fig. 6A-C). Survival analysis showed that the survival rate in the high-risk group was remarkably lower than that in the low-risk group ($p = 8.64e - 10$, Fig. 6D). The area under curve (AUC) of the receiver operating characteristic (ROC) curve was 0.916 (Fig. 6E), suggesting a great performance of the prognostic index model in predicting the prognosis of LSCC patients. Compared with the other clinical factors including only age, gender, grade, stage or TNM, the prognostic index model shown the largest AUC for 1-year, 3-year and 5-year OS (Fig. 7). Moreover, univariate and multiple regression analyses (Fig. 8)

suggested that the prognostic signature could become an independent predictor after adjustment of age, gender, tumor grade, tumor stage, location of the primary tumor(T), distant metastasis(M) and lymph node metastasis status(N) in LSCC patients. In addition, the relationship between IRG expressions and clinical factors of LSCC patients was explored (Fig. 9). In order to assess the prognostic capacity of prognostic index more comprehensively, we conducted a stratified analysis of clinical factors. Interestingly, we found that high risk patients in nearly all the subgroups were inclined to have unfavorable overall survival (Fig. 10).

3.7 Building and validating a predictive nomogram

We used a number of independent prognostic factors (including age, gender, grade,stage,TMN and risk scores) to establish a nomogram to predict 1-year ,3-year and 5-year OS in 88 LSCC patients(Fig. 11).These results suggested that the advantage of a nomogram constructed using a combinatorial model is that it can better predict short-term survival (1-year ,3-year and 5-year OS) compared to a nomogram constructed using a single prognostic factor. This might be helpful for clinical management.

3.8 Identification of the related biological processes and pathways

We used risk score to classify the entire data set to determine the underlying pathway behind these 15 genes by using the Java software GSEA. The results showed that the high-risk group was more abundant in the "glycosaminoglycan biosynthesis keratan sulfate"and"pathogenic escherichia coli infection"gene sets when the low-risk group was more abundant in the "arachidonic acid metabolism","butanoate metabolism","fatty acid metabolism","propanoate metabolism"and "selenoamino acid metabolism"gene sets(Fig. 12).

3.9 Tumor-infiltrating immune cells in LSCC patients of the high-risk and low-risk groups

To explore the relationship between the immunogenomics-based prognostic index model and tumor immune microenvironment, we compared the infiltration of immune cells in different risk groups. It is shown that B cells were significantly enriched in the low-risk group compared to those in the high-risk group(Fig. 13).

4. Discussion

LSCC, a most common tumor of head and neck [19], is prone to recurrence and metastasis[20]. Patients who suffer from recurrent or metastatic LSCC and those with a poor response to platinum-based chemotherapy have a low survival rate [21]. Since the immune system plays a vital role in cancer development, immunotherapy is now extensively applied to counteract the immune escape against malignant cancer cells through regulating the key signaling pathways in the host immune system. In particular, cancer immunotherapy shows potentials of durable responses with fewer adverse effects than conventional treatments [22]. The first cancer immunotherapy drug approved by the Food and Drug Administration (FDA) in 2011 was ipilimumab, a cytotoxic T-lymphocyte antigen 4 (CTLA4)-blocking monoclonal antibody (mAb) for metastatic melanoma.

Although the prognostic models of LSCC for predicting overall survival are constantly updated [23, 24], immune-related prognostic index models of LSCC have rarely been reported. In this study, we first identified 371 up-regulated and 61 down-regulated IRGs of LSCC, and the prognostic IRGs were subsequently screened out. Through establishing a prognostic index model, LSCC patients were classified into the high-risk and the low-risk groups. Our findings demonstrated the great performance of the prognostic index model in predicting the prognosis of LSCC patients as revealed by the ROC curves.

To further explore the biological functions of IRGs in the development of LSCC, pathway enrichment analysis was conducted to depict the regulatory network. The KEGG analysis showed that prognostic IRGs were mainly enriched in the cytokine-cytokine receptor interaction. Immune cells and a network of pro-inflammatory and anti-inflammatory cytokines collaborate in cancer development and progression[25]. Cytokines are a heterogeneous group of soluble, small polypeptides or glycoproteins involved in virtually every aspect of immunity and inflammation [26]. It is believed that an environment rich in inflammatory cells, cytokines and activated stroma potentiates and/or promotes neoplastic risk [27]. Our study also found that the relationships between TFRC, PPARG, AHNAK, TRBC1 and their surrounding TFs were more complex in the regulatory network. TFRC is differentially expressed in tumors[28, 29]. PPARG is considered as a prognostic marker[30, 31]. Our results confirmed that AHNAK acted as a potential tumor suppressor and could be a reliable clinical prognostic indicator[32, 33]. Nevertheless, the potential role of TRBC1 in cancer development remains unclear.

In the constructed prognostic model, the following IRGs were subjected to the calculation of risk score: RBP1, TLR2, PAEP, AHNAK, AQP9, CCL2, PPARG, CYSLTR2, FPR2, BTC, EPO, STC2, TNFRSF4, FCGR3B, PLCG1, AHNAK and PPARG. More frequent methylation of RBP1 is found in the esophageal squamous cell carcinoma than in the normal esophagus [34]. TLR2 may be relevant to susceptibilities of oral squamous cell carcinoma and oral lichenoid lesions[35]. Aquaporins (AQPs), a family of small membrane transport proteins, assist the transportation of water and small solutes such as glycerol [36]. It has been reported that AQP9 is up-regulated in human glioma tissues [37]. In astrocytoma, AQP9 promotes cancer cell invasion and motility via the AKT pathway [38]. Ferreira et al. suggested that CCL2 promoted the spread of oral cavity squamous cell carcinoma to lymph nodes and the macrophage infiltration might play a role in less aggressive behaviors [39]. Cysteinyl-LTs participate in the pathogenesis of several chronic inflammatory diseases [40]. Previous studies found that FPR2-induced paracrine might contribute to the proliferation and metastasis of LSCC [41], which is consistent with our findings. Betacellulin (BTC), a member of the EGF family, acts as a potent mitogen for various cell types[42]. BTC is frequently reported to be up-regulated in human tumors [43–45]. Seibold ND et al. demonstrated that EPO expression in locally advanced squamous cell carcinoma of the head and neck was an independent prognostic factor for locoregional control, metastases-free survival and overall survival[46]. Protein level of STC2 in tumor tissues is associated with invasiveness in the thyroid cartilage, T-stage, lymph node metastasis, clinical stage and pathological differentiation of LSCC. In addition, protein level of STC2 is an independent prognostic factor for overall survival of LSCC [47–49]. Zhu et al. suggested that phospholipase C gamma 1 (PLCG1) could be used as a prognostic biomarker for patients with advanced

oral squamous cell carcinoma[50]. So far, the involvement of PAEP, TNFRSF4 and FCGR3B in LSCC or head and neck tumors remains unclear, which requires further exploration.

T cells contribute to oncological immune defense and B cells basically belong to the adaptive immune system. Currently, most immunotherapies are based on T cells [51]. In this study, we found that B cells were significantly enriched in the low-risk group compared to the high-risk group, suggesting that B cell infiltration might be a good prognostic signal for LSCC patients. B lymphocytes are the effector cells of humoral immunity and can terminally differentiate into antibodies that secrete plasma cells upon stimulation. Moreover, B cells contribute to cellular immunity by acting as antigen-presenting cells (APCs) and/or providing costimulatory signals to T cells [52, 53]. The role of B lymphocytes in tumor immunity is still controversial. On the one hand, antigen-presenting B cells are able to activate tumor-specific cytotoxic T cells [54]. B cell deficient mice exhibit significantly reduced tumor-specific T cell immunity [55]. On the other hand, B cell antibody response may potentiate chronic inflammation and thus enhance tumor development [56, 57]. It is reported that tumor infiltrating B-cells are correlated with a good prognosis for head and neck cancer [58], which is consistent with our findings.

There are still some deficiencies in our study. First of all, we constructed a unique prognostic model of LSCC by analyzing IRGs. However, in-depth analyses on clinical data of LSCC patients are needed to confirm our findings. Secondly, we did not monitor the relative expressions of the selected 15 IRGs in LSCC patients to assess their prognostic values. Thirdly, *in vivo* and *in vitro* functional experiments are needed to further validate our findings.

5. Conclusions

We developed a novel IRGs-based prognostic index model for LSCC patients, an interpretation of the mis-regulated tumor immune microenvironment. Also, these IRGs could be the potential therapeutic targets for LSCC patients.

Abbreviations

LSCC:Laryngeal squamous cell carcinoma

IRGs:Immune-related genes

TCGA:The Cancer Genome Atlas

TFs:Transcription factors

FDR:False discovery rate

GO:Gene Ontology

KEGG:Kyoto Encyclopedia of Genes and Genomes

ROC:Receiver operating characteristic

AUC:Area under curve

THPA:The Human Protein Atlas

Declarations

Availability of data and materials

The raw datasets analyzed during the current study are available from the corresponding author on reasonable request.

Ethics approval and consent to participate.

Not applicable.

Consent for publication.

Not applicable.

Availability of data and materials.

The datasets used and/or analysed during the current study are available from the corresponding author on reasonable request.

Competing interests.

The authors declare that they have no competing interests.

Funding.

This study was supported by the Research Grant from Jiangsu Provincial Commission of Health (H201603), and the Health Promotion Project (QNRC2016614) of Jiangsu Province, the People's Republic of China. Both grants provided fundamental support for the bioinformatic data analysis, statistical clinical data investigation and manuscript preparations.

Authors' contributions.

Yujie Shen, Han Zhou and Shikun Dong contributed equally to this study.

Acknowledgements.

This study was supported by the Research Grant from Jiangsu Provincial Commission of Health (H201603), and the Health Promotion Project (QNRC2016614) of Jiangsu Province, the People's Republic of China.

References

1. Marioni G, Marchese-Ragona R, Cartei G, Marchese F, Staffieri A: **Current opinion in diagnosis and treatment of laryngeal carcinoma.** *Cancer Treat Rev* 2006, **32**(7):504-515.
2. Hardisson D: **Molecular pathogenesis of head and neck squamous cell carcinoma.** *Eur Arch Otorhinolaryngol* 2003, **260**(9):502-508.
3. Suh Y, Amelio I, Guerrero Urbano T, Tavassoli M: **Clinical update on cancer: molecular oncology of head and neck cancer.** *Cell Death Dis* 2014, **5**:e1018.
4. Li B, Cui Y, Diehn M, Li R: **Development and Validation of an Individualized Immune Prognostic Signature in Early-Stage Nonsquamous Non-Small Cell Lung Cancer.** *JAMA Oncol* 2017, **3**(11):1529-1537.
5. Lin P, Guo YN, Shi L, Li XJ, Yang H, He Y, Li Q, Dang YW, Wei KL, Chen G: **Development of a prognostic index based on an immunogenomic landscape analysis of papillary thyroid cancer.** *Aging (Albany NY)* 2019, **11**(2):480-500.
6. Kadota K, Nitadori JI, Ujiie H, Buitrago DH, Woo KM, Sima CS, Travis WD, Jones DR, Adusumilli PS: **Prognostic Impact of Immune Microenvironment in Lung Squamous Cell Carcinoma: Tumor-Infiltrating CD10+ Neutrophil/CD20+ Lymphocyte Ratio as an Independent Prognostic Factor.** *J Thorac Oncol* 2015, **10**(9):1301-1310.
7. Dahlin AM, Henriksson ML, Van Guelpen B, Stenling R, Oberg A, Rutegard J, Palmqvist R: **Colorectal cancer prognosis depends on T-cell infiltration and molecular characteristics of the tumor.** *Mod Pathol* 2011, **24**(5):671-682.
8. Adams S, Gray RJ, Demaria S, Goldstein L, Perez EA, Shulman LN, Martino S, Wang M, Jones VE, Saphner TJ *et al*: **Prognostic value of tumor-infiltrating lymphocytes in triple-negative breast cancers from two phase III randomized adjuvant breast cancer trials: ECOG 2197 and ECOG 1199.** *J Clin Oncol* 2014, **32**(27):2959-2966.
9. Lee JS: **Exploring cancer genomic data from the cancer genome atlas project.** *BMB Rep* 2016, **49**(11):607-611.
10. Bhattacharya S, Dunn P, Thomas CG, Smith B, Schaefer H, Chen J, Hu Z, Zalocusky KA, Shankar RD, Shen-Orr SS *et al*: **ImmPort, toward repurposing of open access immunological assay data for translational and clinical research.** *Sci Data* 2018, **5**:180015.
11. Mei S, Meyer CA, Zheng R, Qin Q, Wu Q, Jiang P, Li B, Shi X, Wang B, Fan J *et al*: **Cistrome Cancer: A Web Resource for Integrative Gene Regulation Modeling in Cancer.** *Cancer Res* 2017, **77**(21):e19-e22.
12. Li T, Fan J, Wang B, Traugh N, Chen Q, Liu JS, Li B, Liu XS: **TIMER: A Web Server for Comprehensive Analysis of Tumor-Infiltrating Immune Cells.** *Cancer Res* 2017, **77**(21):e108-e110.
13. Silva TS, Richard N: **Visualization and Differential Analysis of Protein Expression Data Using R.** *Methods Mol Biol* 2016, **1362**:105-118.
14. Shannon P, Markiel A, Ozier O, Baliga NS, Wang JT, Ramage D, Amin N, Schwikowski B, Ideker T: **Cytoscape: a software environment for integrated models of biomolecular interaction networks.**

Genome Res 2003, **13**(11):2498-2504.

15. Clough E, Barrett T: **The Gene Expression Omnibus Database.** *Methods Mol Biol* 2016, **1418**:93-110.
16. Thul PJ, Lindskog C: **The human protein atlas: A spatial map of the human proteome.** *Protein Sci* 2018, **27**(1):233-244.
17. Kamarudin AN, Cox T, Kolamunnage-Dona R: **Time-dependent ROC curve analysis in medical research: current methods and applications.** *BMC Med Res Methodol* 2017, **17**(1):53.
18. Subramanian A, Tamayo P, Mootha VK, Mukherjee S, Ebert BL, Gillette MA, Paulovich A, Pomeroy SL, Golub TR, Lander ES *et al*: **Gene set enrichment analysis: a knowledge-based approach for interpreting genome-wide expression profiles.** *Proc Natl Acad Sci U S A* 2005, **102**(43):15545-15550.
19. Steuer CE, El-Deiry M, Parks JR, Higgins KA, Saba NF: **An update on larynx cancer.** *CA Cancer J Clin* 2017, **67**(1):31-50.
20. Obid R, Redlich M, Tomeh C: **The Treatment of Laryngeal Cancer.** *Oral Maxillofac Surg Clin North Am* 2019, **31**(1):1-11.
21. Saloura V, Cohen EE, Licitra L, Billan S, Dinis J, Lisby S, Gauler TC: **An open-label single-arm, phase II trial of zalutumumab, a human monoclonal anti-EGFR antibody, in patients with platinum-refractory squamous cell carcinoma of the head and neck.** *Cancer Chemother Pharmacol* 2014, **73**(6):1227-1239.
22. Moy JD, Moskovitz JM, Ferris RL: **Biological mechanisms of immune escape and implications for immunotherapy in head and neck squamous cell carcinoma.** *Eur J Cancer* 2017, **76**:152-166.
23. Yang L, Hong S, Wang Y, He Z, Liang S, Chen H, He S, Wu S, Song L, Chen Y: **A novel prognostic score model incorporating CDGSH iron sulfur domain2 (CISD2) predicts risk of disease progression in laryngeal squamous cell carcinoma.** *Oncotarget* 2016, **7**(16):22720-22732.
24. Te Riele R, Dronkers EAC, Wieringa MH, De Herdt MJ, Sewnaik A, Hardillo JA, Baatenburg de Jong RJ: **Influence of anemia and BMI on prognosis of laryngeal squamous cell carcinoma: Development of an updated prognostic model.** *Oral Oncol* 2018, **78**:25-30.
25. Seruga B, Zhang H, Bernstein LJ, Tannock IF: **Cytokines and their relationship to the symptoms and outcome of cancer.** *Nat Rev Cancer* 2008, **8**(11):887-899.
26. Borish LC, Steinke JW: **2. Cytokines and chemokines.** *J Allergy Clin Immunol* 2003, **111**(2 Suppl):S460-475.
27. Balkwill F, Mantovani A: **Inflammation and cancer: back to Virchow?** *Lancet* 2001, **357**(9255):539-545.
28. Wada S, Noguchi T, Takeno S, Kawahara K: **PIK3CA and TFRC located in 3q are new prognostic factors in esophageal squamous cell carcinoma.** *Ann Surg Oncol* 2006, **13**(7):961-966.
29. Jhaveri DT, Kim MS, Thompson ED, Huang L, Sharma R, Klein AP, Zheng L, Le DT, Laheru DA, Pandey A *et al*: **Using Quantitative Seroproteomics to Identify Antibody Biomarkers in Pancreatic Cancer.** *Cancer Immunol Res* 2016, **4**(3):225-233.

30. Ahmad I, Mui E, Galbraith L, Patel R, Tan EH, Salji M, Rust AG, Repiscak P, Hedley A, Markert E *et al*: **Sleeping Beauty screen reveals Pparg activation in metastatic prostate cancer.** *Proc Natl Acad Sci U S A* 2016, **113**(29):8290-8295.
31. Goldstein JT, Berger AC, Shih J, Duke FF, Furst L, Kwiatkowski DJ, Cherniack AD, Meyerson M, Strathdee CA: **Genomic Activation of PPARG Reveals a Candidate Therapeutic Axis in Bladder Cancer.** *Cancer Res* 2017, **77**(24):6987-6998.
32. Zhao Z, Xiao S, Yuan X, Yuan J, Zhang C, Li H, Su J, Wang X, Liu Q: **AHNAK as a Prognosis Factor Suppresses the Tumor Progression in Glioma.** *J Cancer* 2017, **8**(15):2924-2932.
33. Chen B, Wang J, Dai D, Zhou Q, Guo X, Tian Z, Huang X, Yang L, Tang H, Xie X: **AHNAK suppresses tumour proliferation and invasion by targeting multiple pathways in triple-negative breast cancer.** *J Exp Clin Cancer Res* 2017, **36**(1):65.
34. Tsunoda S, Smith E, De Young NJ, Wang X, Tian ZQ, Liu JF, Jamieson GG, Drew PA: **Methylation of CLDN6, FBN2, RBP1, RBP4, TFPI2, and TMEFF2 in esophageal squamous cell carcinoma.** *Oncol Rep* 2009, **21**(4):1067-1073.
35. de Barros Gallo C, Marichalar-Mendia X, Setien-Olarra A, Acha-Sagredo A, Bediaga NG, Gainza-Cirauqui ML, Sugaya NN, Aguirre-Urizar JM: **Toll-like receptor 2 rs4696480 polymorphism and risk of oral cancer and oral potentially malignant disorder.** *Arch Oral Biol* 2017, **82**:109-114.
36. Agre P, King LS, Yasui M, Guggino WB, Ottersen OP, Fujiyoshi Y, Engel A, Nielsen S: **Aquaporin water channels—from atomic structure to clinical medicine.** *J Physiol* 2002, **542**(Pt 1):3-16.
37. Warth A, Mittelbronn M, Hulper P, Erdlenbruch B, Wolburg H: **Expression of the water channel protein aquaporin-9 in malignant brain tumors.** *Appl Immunohistochem Mol Morphol* 2007, **15**(2):193-198.
38. Lv Y, Huang Q, Dai W, Jie Y, Yu G, Fan X, Wu A, Miao Q: **AQP9 promotes astrocytoma cell invasion and motility via the AKT pathway.** *Oncol Lett* 2018, **16**(5):6059-6064.
39. Ferreira FO, Ribeiro FL, Batista AC, Leles CR, de Cassia Goncalves Alencar R, Silva TA: **Association of CCL2 with lymph node metastasis and macrophage infiltration in oral cavity and lip squamous cell carcinoma.** *Tumour Biol* 2008, **29**(2):114-121.
40. Samuelsson B: **Leukotrienes: a new class of mediators of immediate hypersensitivity reactions and inflammation.** *Adv Prostaglandin Thromboxane Leukot Res* 1983, **11**:1-13.
41. Gastardelo TS, Cunha BR, Raposo LS, Maniglia JV, Cury PM, Lisoni FC, Tajara EH, Olini SM: **Inflammation and cancer: role of annexin A1 and FPR2/ALX in proliferation and metastasis in human laryngeal squamous cell carcinoma.** *PLoS One* 2014, **9**(12):e111317.
42. Schneider MR, Wolf E: **The epidermal growth factor receptor ligands at a glance.** *J Cell Physiol* 2009, **218**(3):460-466.
43. Zhao J, Klausen C, Qiu X, Cheng JC, Chang HM, Leung PC: **Betacellulin induces Slug-mediated down-regulation of E-cadherin and cell migration in ovarian cancer cells.** *Oncotarget* 2016, **7**(20):28881-28890.
44. Shi L, Wang L, Wang B, Cretoiu SM, Wang Q, Wang X, Chen C: **Regulatory mechanisms of betacellulin in CXCL8 production from lung cancer cells.** *J Transl Med* 2014, **12**:70.

45. Byeon SJ, Lee HS, Kim MA, Lee BL, Kim WH: **Expression of the ERBB Family of Ligands and Receptors in Gastric Cancer.** *Pathobiology* 2017, **84**(4):210-217.
46. Seibold ND, Schild SE, Gebhard MP, Noack F, Schroder U, Rades D: **Prognosis of patients with locally advanced squamous cell carcinoma of the head and neck. Impact of tumor cell expression of EPO and EPO-R.** *Strahlenther Onkol* 2013, **189**(7):559-565.
47. Zhang C, Guan Z, Peng J: **[The correlation between stanniocalcin 2 expression and prognosis in laryngeal squamous cell cancer].** *Lin Chung Er Bi Yan Hou Tou Jing Wai Ke Za Zhi* 2015, **29**(2):102-107.
48. Zhou H, Li YY, Zhang WQ, Lin D, Zhang WM, Dong WD: **Expression of stanniocalcin-1 and stanniocalcin-2 in laryngeal squamous cell carcinoma and correlations with clinical and pathological parameters.** *PLoS One* 2014, **9**(4):e95466.
49. Kong X, Qi J, Yan Y, Chen L, Zhao Y, Fang Z, Fan J, Liu M, Liu Y: **Comprehensive analysis of differentially expressed profiles of lncRNAs, mRNAs, and miRNAs in laryngeal squamous cell carcinoma in order to construct a ceRNA network and identify potential biomarkers.** *J Cell Biochem* 2019, **120**(10):17963-17974.
50. Zhu D, Tan Y, Yang X, Qiao J, Yu C, Wang L, Li J, Zhang Z, Zhong L: **Phospholipase C gamma 1 is a potential prognostic biomarker for patients with locally advanced and resectable oral squamous cell carcinoma.** *Int J Oral Maxillofac Surg* 2014, **43**(12):1418-1426.
51. Zhang Y, Gallastegui N, Rosenblatt JD: **Regulatory B cells in anti-tumor immunity.** *Int Immunol* 2015, **27**(10):521-530.
52. Bouaziz JD, Yanaba K, Venturi GM, Wang Y, Tisch RM, Poe JC, Tedder TF: **Therapeutic B cell depletion impairs adaptive and autoreactive CD4+ T cell activation in mice.** *Proc Natl Acad Sci U S A* 2007, **104**(52):20878-20883.
53. Crawford A, Macleod M, Schumacher T, Corlett L, Gray D: **Primary T cell expansion and differentiation in vivo requires antigen presentation by B cells.** *J Immunol* 2006, **176**(6):3498-3506.
54. Coughlin CM, Vance BA, Grupp SA, Vonderheide RH: **RNA-transfected CD40-activated B cells induce functional T-cell responses against viral and tumor antigen targets: implications for pediatric immunotherapy.** *Blood* 2004, **103**(6):2046-2054.
55. Schultz KR, Klarnet JP, Gieni RS, HayGlass KT, Greenberg PD: **The role of B cells for in vivo T cell responses to a Friend virus-induced leukemia.** *Science* 1990, **249**(4971):921-923.
56. de Visser KE, Korets LV, Coussens LM: **De novo carcinogenesis promoted by chronic inflammation is B lymphocyte dependent.** *Cancer Cell* 2005, **7**(5):411-423.
57. Houghton AN, Uchi H, Wolchok JD: **The role of the immune system in early epithelial carcinogenesis: B-ware the double-edged sword.** *Cancer Cell* 2005, **7**(5):403-405.
58. Pretscher D, Distel LV, Grabenbauer GG, Wittlinger M, Buettner M, Niedobitek G: **Distribution of immune cells in head and neck cancer: CD8+ T-cells and CD20+ B-cells in metastatic lymph nodes are associated with favourable outcome in patients with oro- and hypopharyngeal carcinoma.** *BMC Cancer* 2009, **9**:292.

Tables

Due to technical limitations the Tables are available as downloads in the Supplementary Files>

Figures

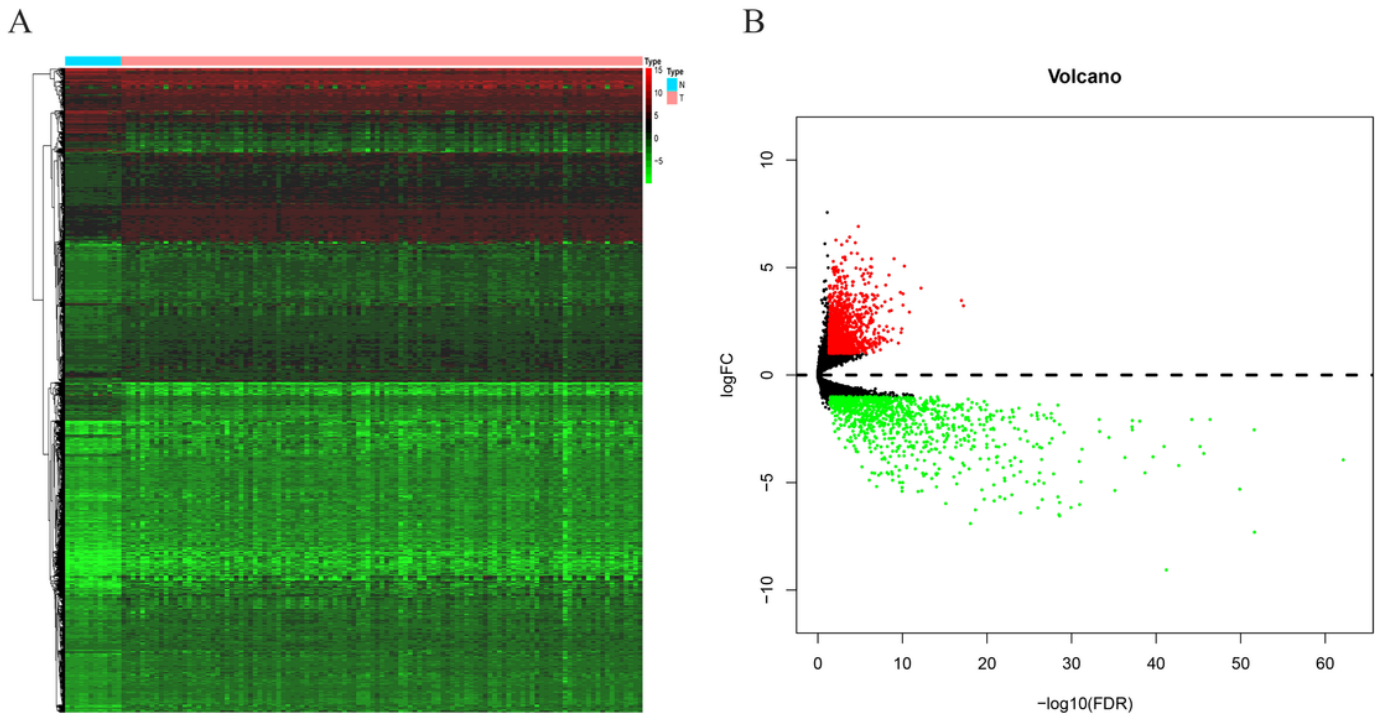


Figure 1

Heatmap and volcanic maps of 5483 DEGs. A: Red: up-regulation; Green: down-regulation. B: Red and green plots: differentially expressed mRNAs as indicated in A; Black plots: normally expressed mRNAs

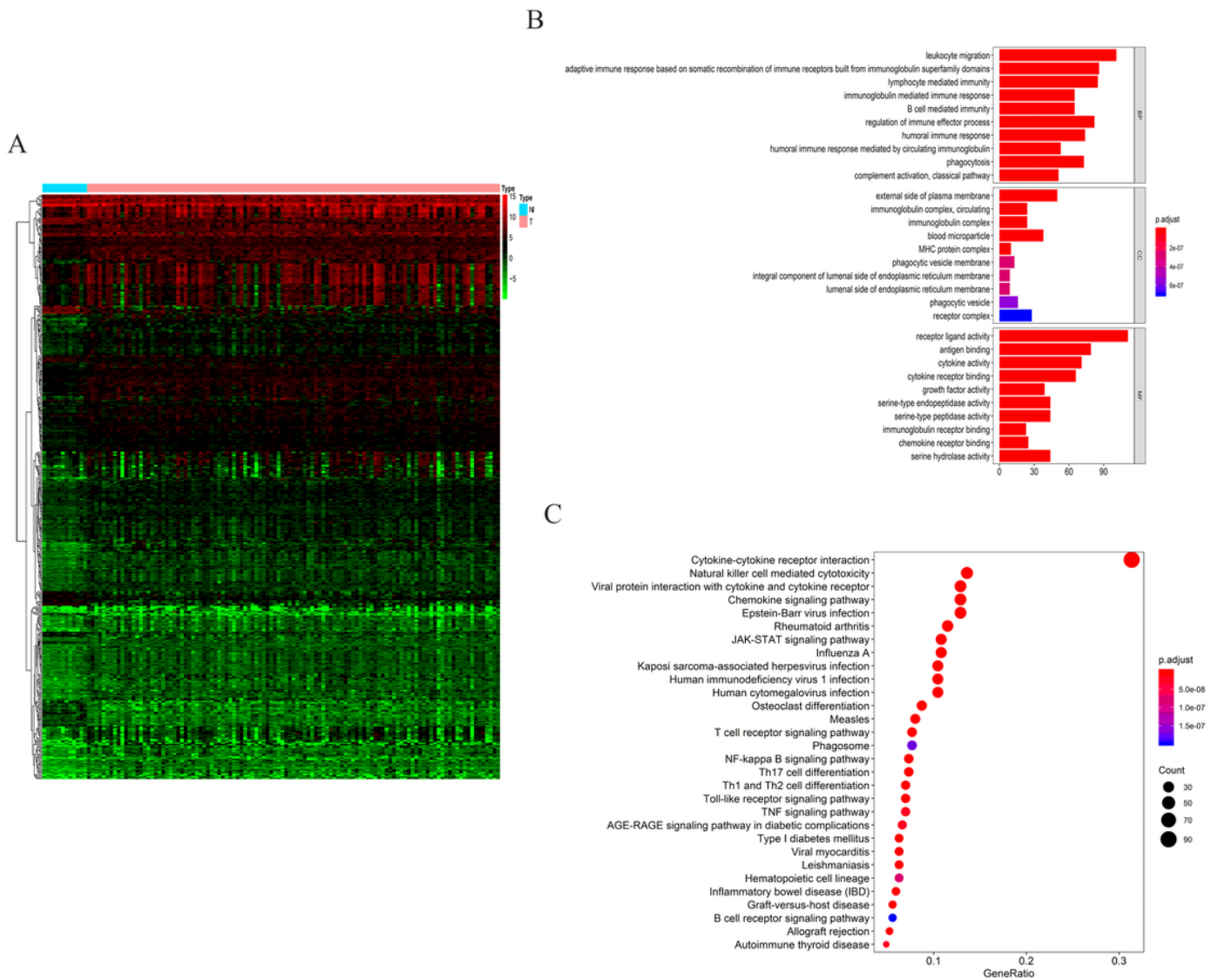


Figure 2

Cluster analysis and gene enrichment analysis of IRGs. A: Heatmap of 432 IRGs. B: Significantly enriched GO terms of IRGs. C: Significant KEGG pathway terms of IRGs

	pvalue	Hazard ratio
CXCL11	0.015	1.016(1.003-1.030)
RBP1	0.013	1.007(1.001-1.012)
TLR2	0.004	1.036(1.011-1.061)
PAEP	0.027	1.112(1.012-1.222)
TFRC	0.026	1.007(1.001-1.014)
VEGFA	0.029	0.945(0.898-0.994)
AHNAK	0.026	1.007(1.001-1.013)
AQP9	0.005	1.091(1.026-1.160)
CCL2	0.047	1.024(1.000-1.048)
XCL2	0.030	0.387(0.164-0.911)
PPARG	0.045	1.219(1.004-1.481)
PROK2	0.031	1.156(1.013-1.320)
CYSLTR2	0.027	0.282(0.092-0.865)
FPR2	0.041	1.309(1.011-1.695)
BTC	0.006	1.518(1.126-2.046)
EPO	0.014	0.357(0.157-0.813)
PDGFA	0.017	1.058(1.010-1.108)
PDGFB	0.028	1.062(1.006-1.120)
STC2	<0.001	1.048(1.022-1.074)
IL13RA2	0.002	1.106(1.037-1.179)
IL31RA	0.017	1.483(1.073-2.050)
TNFRSF25	0.019	0.854(0.749-0.974)
TNFRSF4	0.031	0.835(0.708-0.984)
TUBB3	0.006	1.392(1.098-1.764)
LCK	0.011	0.842(0.738-0.962)
FCGR3B	0.048	1.150(1.001-1.321)
ZAP70	0.008	0.683(0.514-0.906)
PLCG1	0.007	0.815(0.703-0.946)
TRBC1	0.050	0.352(0.124-0.999)
TRBJ2-3	0.010	0.459(0.254-0.827)

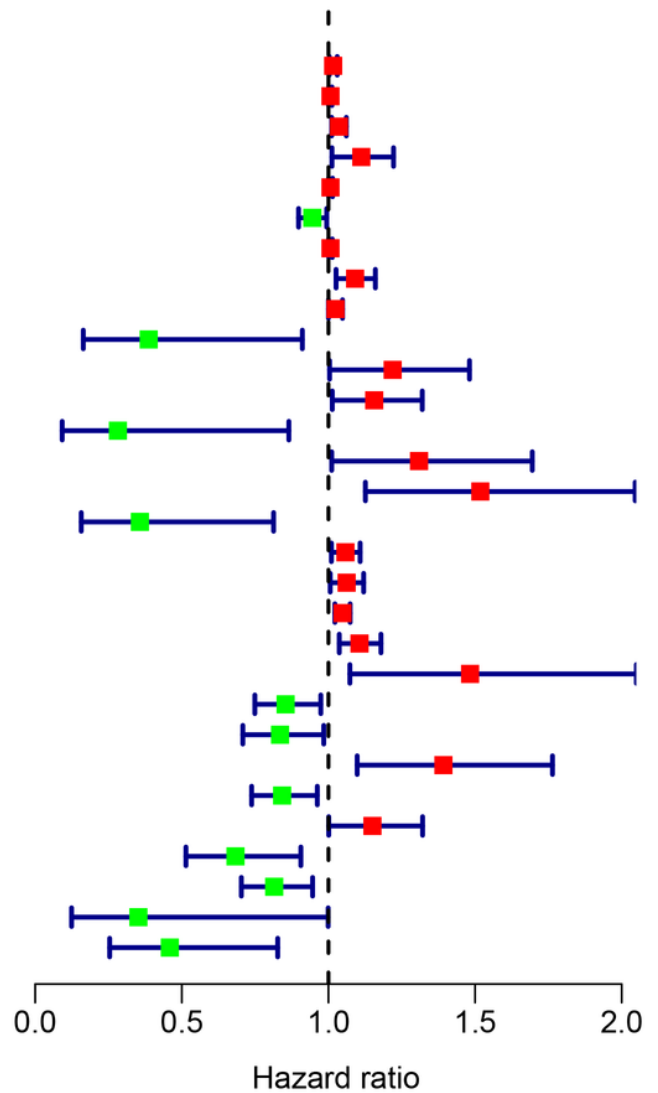
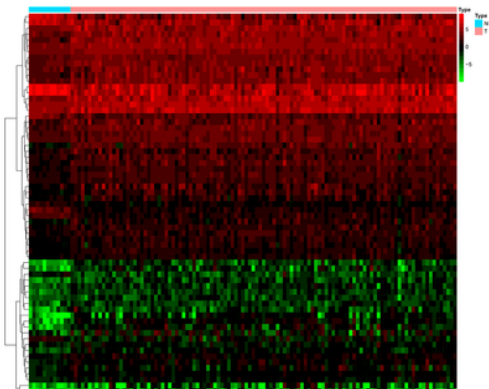


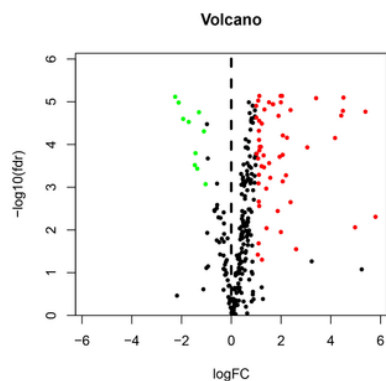
Figure 3

Expression profiles and prognostic values of IRGs

A



B



C

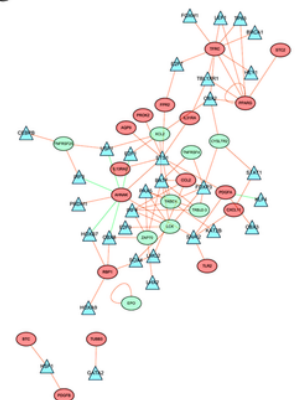


Figure 4

Differential expression analysis of TFs and the regulatory network. A: Heatmap of TFs, Red: up-regulation; Green: down-regulation. B: Volcanic maps of TFs, red and green plots: differentially expressed mRNAs as indicated in A; Black plots: normally expressed mRNAs. C: Regulatory network integrated the IRGs and relevant TFs

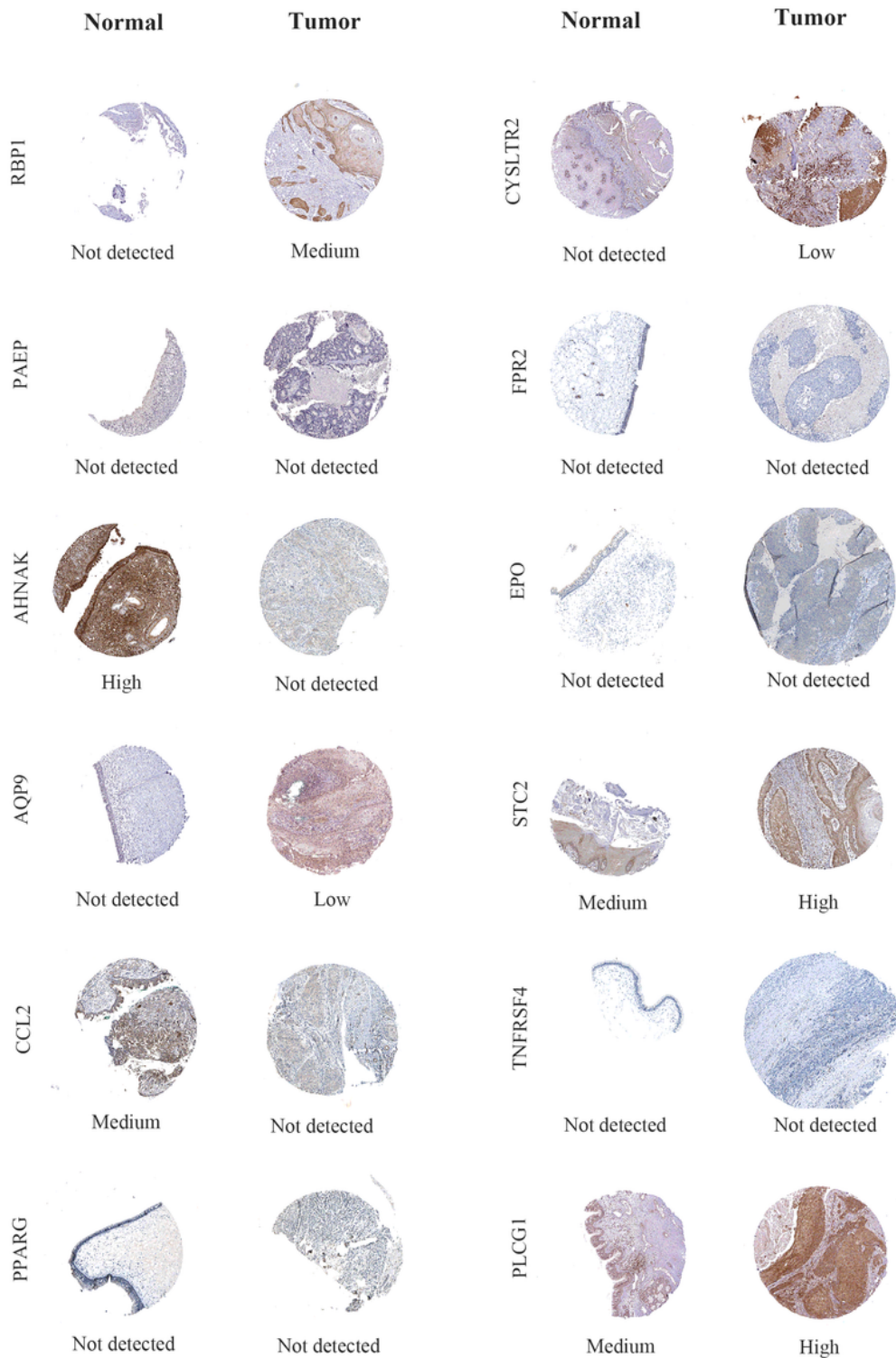


Figure 5

Protein expression of genes in the model

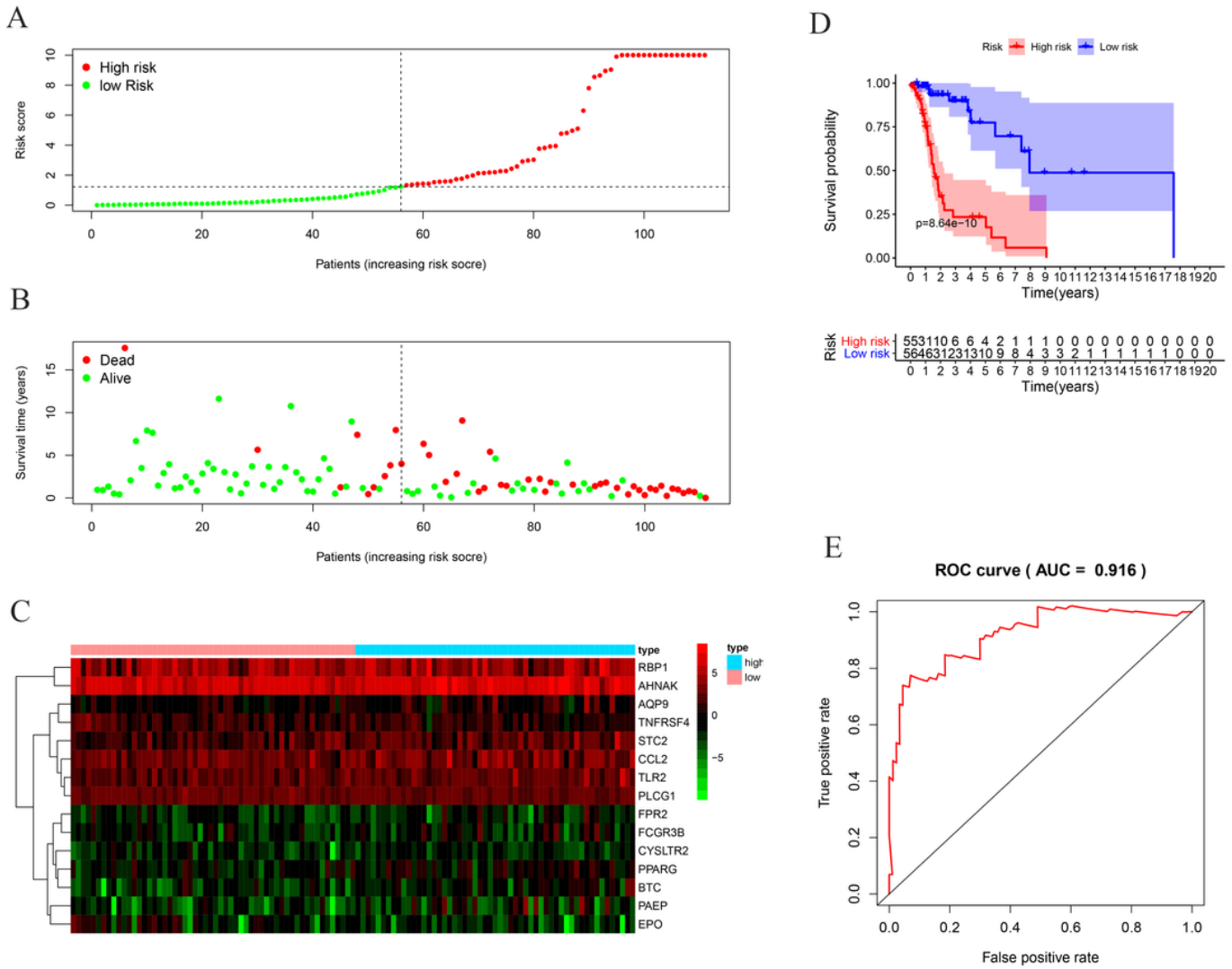


Figure 6

The prognostic value of prognostic index based on IRGs. A: Rank of prognostic index and distribution of groups. B: Survival status of patients in different groups. C: Heatmap of expression profiles of included IRGs. D: Survival analysis between the two groups. E: ROC curve of the prognostic index model .

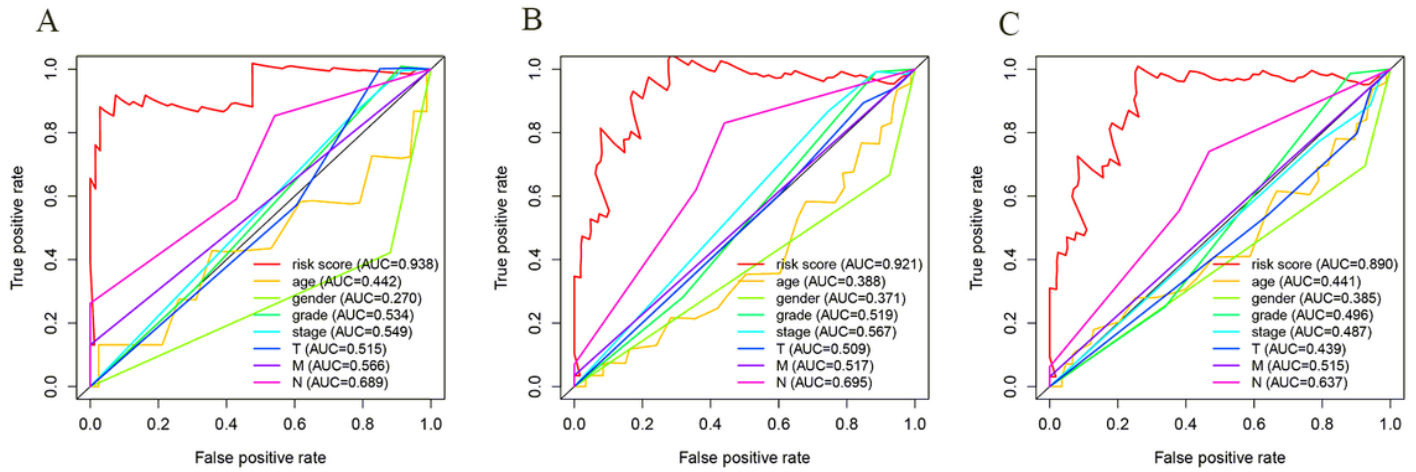


Figure 7

ROC curve of the prognostic index model compared with the other clinical factors. A: AUC for 1-year; B: AUC for 3-year; C: AUC for 5-year.

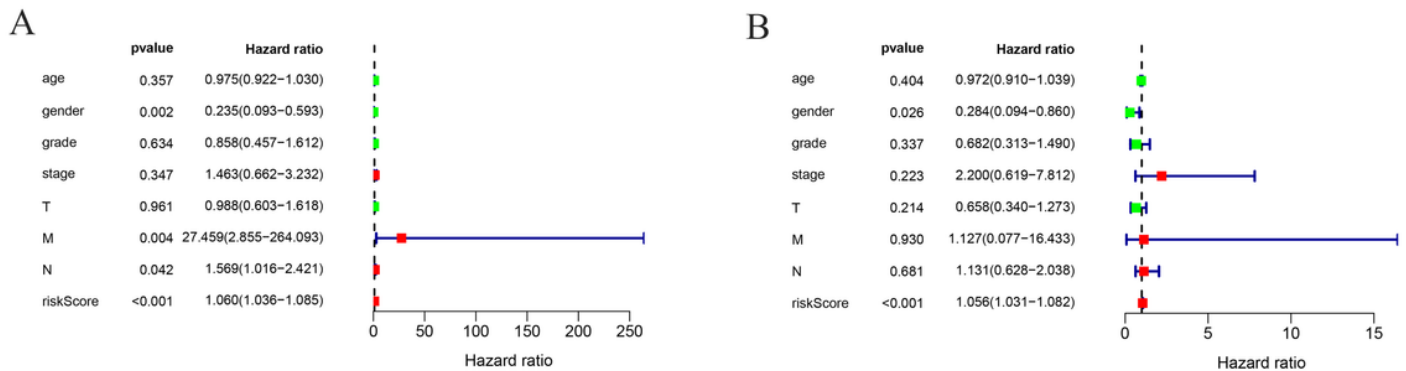


Figure 8

Forest plots including the risk score and other clinical parameters by univariate (A) and multiple regression analysis (B).

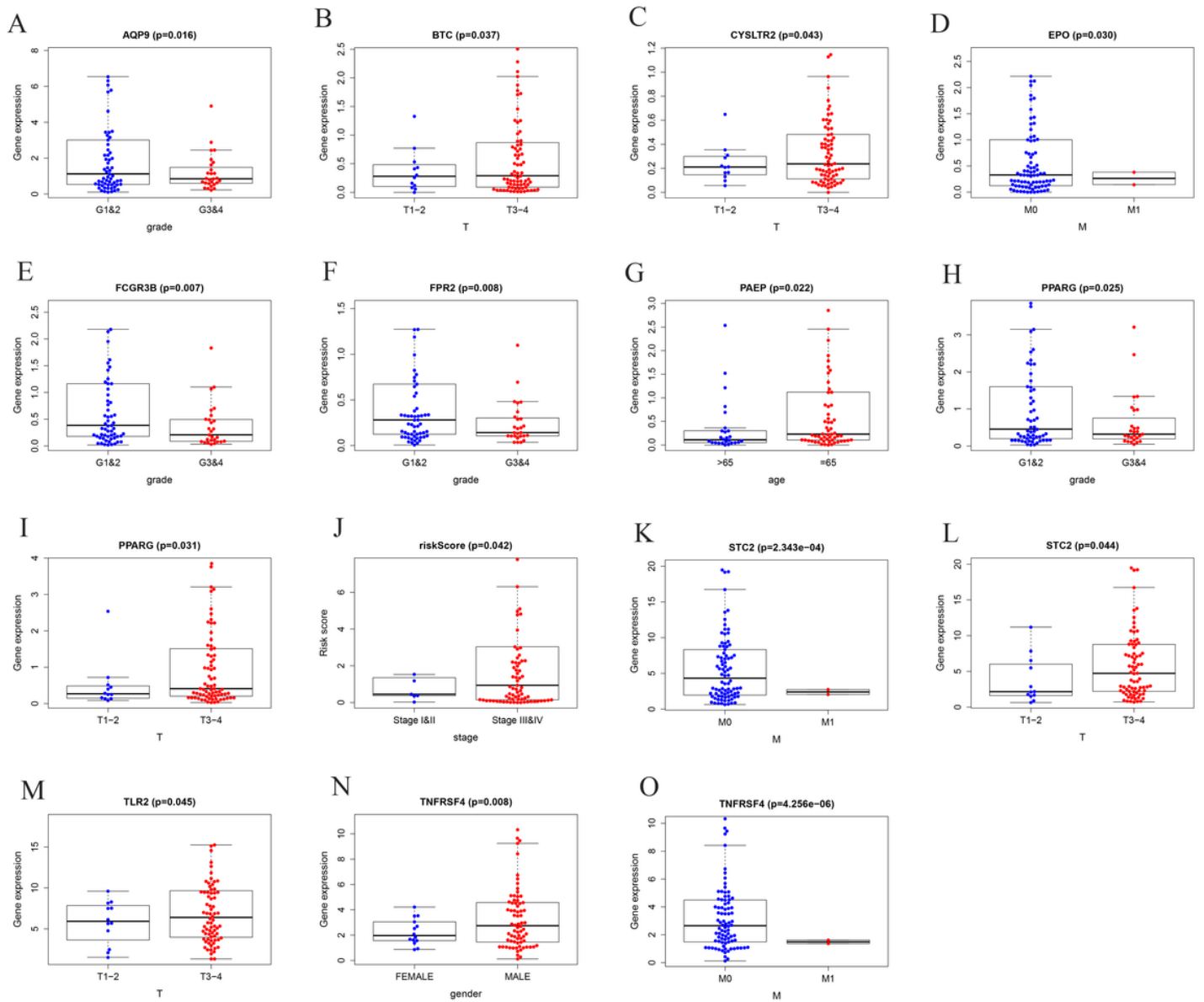


Figure 9

Different expression between the IRGs in prognostic index model and the clinical factors.

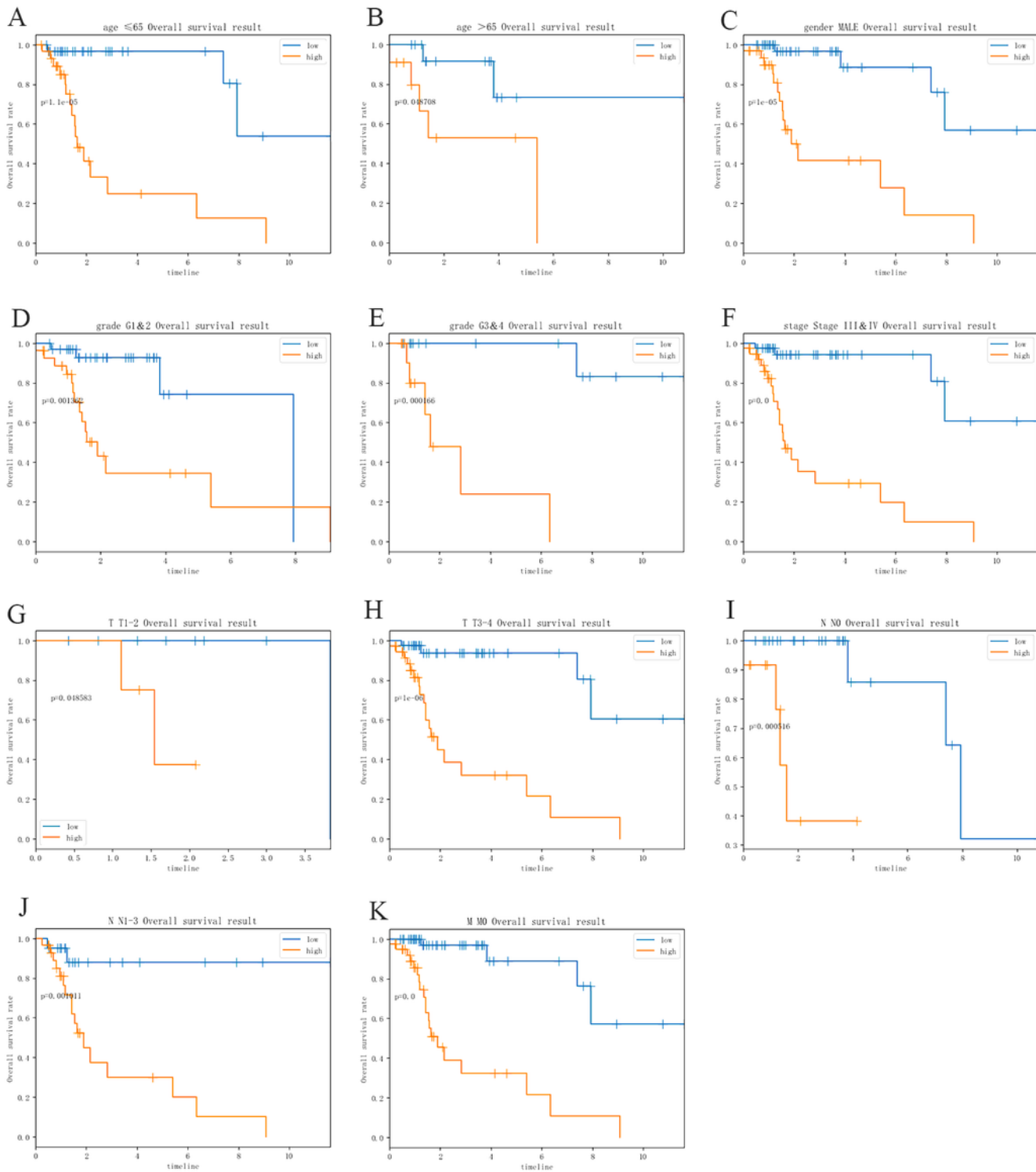
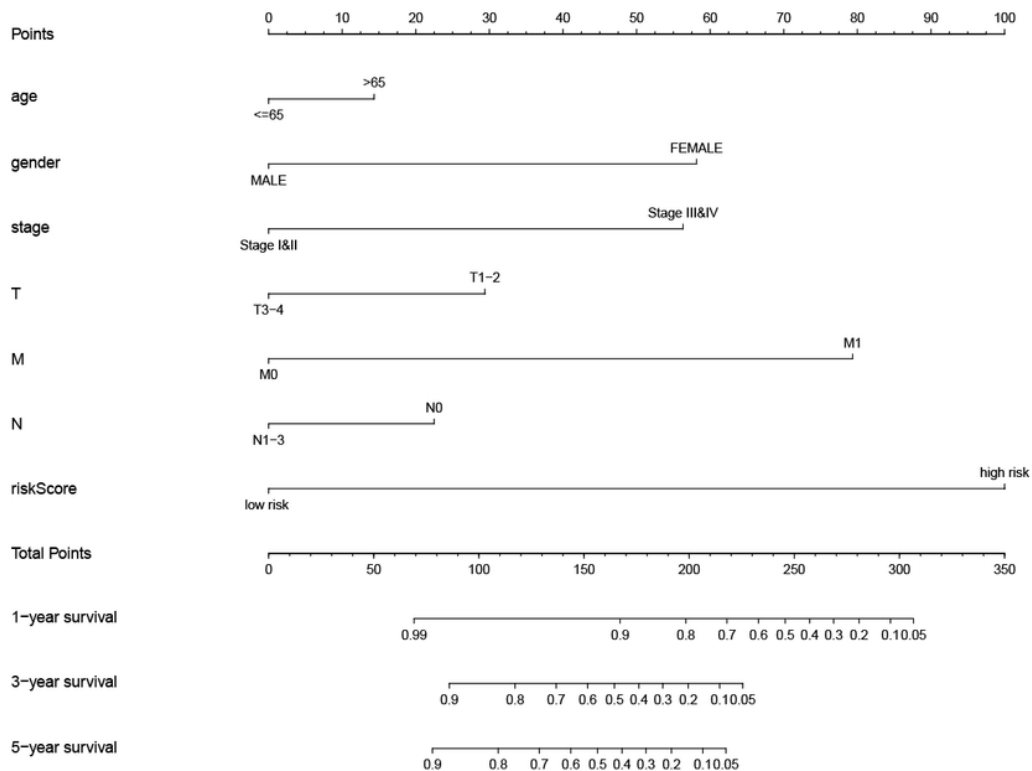


Figure 10

Subgroup survival analysis for patients with LSCC according to the prognostic index stratified by clinical factors.(A) age ≤ 65 ; (B) age > 65 ; (C)gender MALE; (D) grade G1&2; (E)grade G3&4 ; (F)stage III&IV ; (G)T1-2; (H) T3-4;(I):N0;(J):N1-3;(K):M0.

A



B

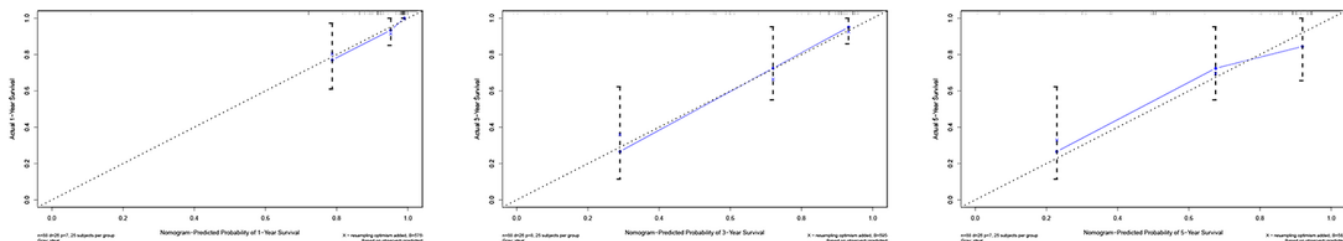


Figure 11

Nomogram predicting overall survival for LSCC patients. A: For each patient, several lines are drawn upward to determine the points received from the predictors in the nomogram. The sum of these points is on the "total point" axis. Then a line is drawn downward to determine the possibility of 1-,3- and 5-year overall survival of LSCC. B: The calibration plot for internal validation of the nomogram. The Y-axis represents actual survival, and the X-axis represents nomogram-predicted survival.

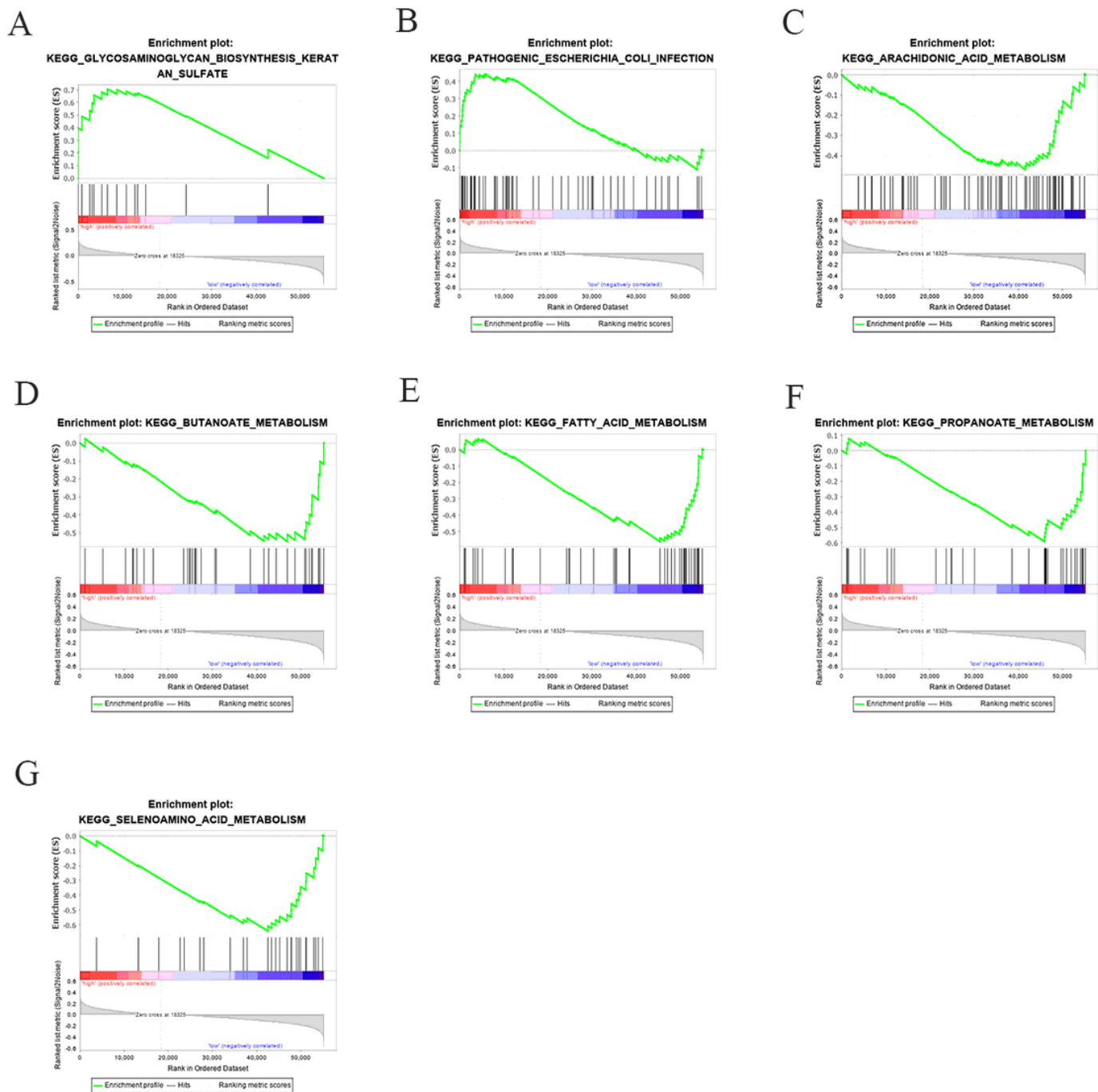


Figure 12

The results of GSEA for high and low risk differentially expressed genes in TCGA. A: glycosaminoglycan biosynthesis keratan sulfate; B: pathogenic escherichia coli infection; C: arachidonic acid metabolism; D: butanoate metabolism; E: fatty acid metabolism; F: propanoate metabolism; G: selenoamino acid metabolism.

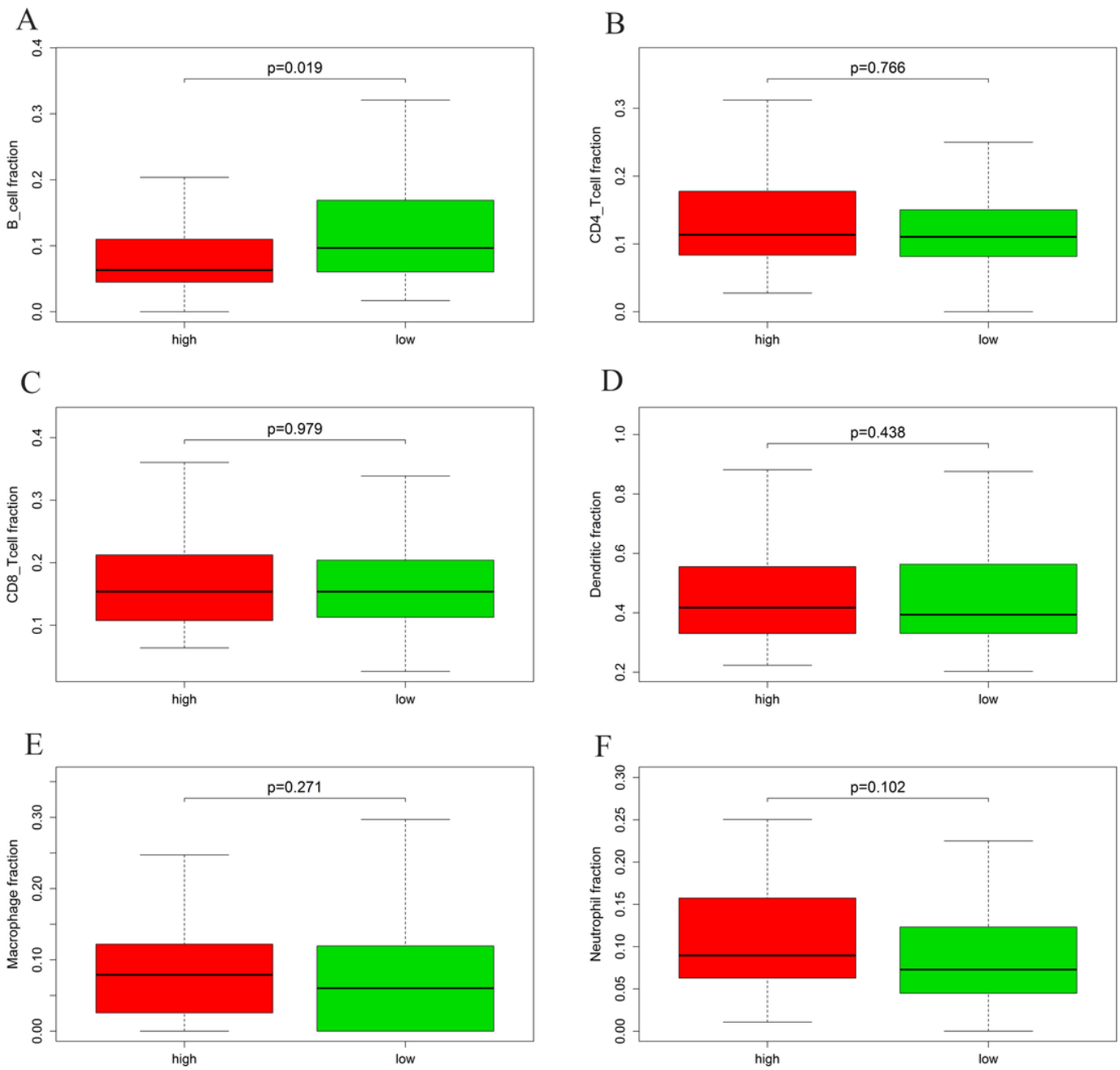


Figure 13

Relationship between the immune-related prognostic index and the infiltration abundances of six types of immune cells. A: B cell; B: CD4 T cell; C: CD8 T cell; D: Dendritic; E: Macrophage; F: Neutrophil.

Supplementary Files

This is a list of supplementary files associated with this preprint. Click to download.

- [Table1.xlsx](#)

- [Table2.xls](#)
- [Table3.xls](#)